

Thoracic Infections in Immunocompromised Patients

Ruchi Sharma¹ · Jeffrey P. Kanne¹ · Maria D. Martin¹ · Christopher A. Meyer¹

Published online: 27 February 2018
© Springer Science+Business Media, LLC, part of Springer Nature 2018

Abstract

Purpose of Review The purpose of this review is to summarize the imaging findings of thoracic infections occurring in immunocompromised patients. Lung infection remains one of the most common complications in immunocompromised patients and is one of the major contributors to morbidity and mortality. Imaging examinations are frequently performed in immunocompromised patients suspected of having chest infection. This review primarily illustrates the CT findings of lung infection. Early detection is important because these patients can rapidly develop fulminant disease.

Recent Findings The imaging findings of a variety of pulmonary infections have been described, and it is well recognized that there is significant overlap of imaging findings across a variety of infections. However, the presence or absence of certain findings can favor one type of infection over another, especially when clinical factors are taken into consideration.

Summary Radiologists play a central role in identifying chest infections in immunocompromised patients. Knowledge of the association between specific infections and specific types of immunodeficiency can aid the radiologist in providing a focused differential diagnosis. Furthermore, knowledge of noninfectious complications such as drug reaction or neoplasm can help guide patient management.

Keywords Immunocompromised · Opportunistic infection · Pneumonia · Transplant · HIV · Computed tomography

Introduction

The number of immunocompromised patients is increasing as a result of expanded use of immunosuppressive therapies for hematologic and solid organ malignancies, autoimmune diseases, and prolonged survival in solid and hematopoietic stem cell transplant recipients [1–3]. Furthermore, human immunodeficiency virus (HIV) infection still accounts for a large number of immunocompromised patients, especially in the developing world. Due to direct communication of the respiratory system with the environment, pulmonary infections are among the most frequent complications affecting immunocompromised patients and are major contributors to morbidity and mortality [4].

A broad range of pathogens, both opportunistic and community acquired, affect immunocompromised patients, with specific susceptibilities depending on type and severity of immune dysfunction. Infection with more than one pathogen is not uncommon [5]. Early detection of pulmonary infection in immunocompromised patients is important because signs and symptoms of infection may be subtle as a result of blunted immune response, and infection can rapidly progress into fulminant illness [3].

This article illustrates the imaging findings of thoracic infection in the most commonly encountered types of immunocompromised patients, focusing on imaging patterns and their associated differential diagnoses including noninfectious causes (Table 1). The intent is to help the reader integrate the imaging findings with the clinical setting in order to generate a clinically relevant differential diagnosis (Table 2).

This article is part of the Topical collection on *Chest Imaging*.

✉ Jeffrey P. Kanne
jkanne@uwhealth.org

¹ Department of Radiology, University of Wisconsin School of Medicine and Public Health, 600 Highland Avenue, Madison, WI 53792, USA

Imaging

Chest radiography is the preferred initial diagnostic imaging examination for evaluation of suspected chest infection in immunocompromised patients because of its relative low cost, widespread availability, and minimal radiation dose. Due to the blunted host immune response, radiographic findings may be subtle or occult until more widespread infection has developed. [1, 6••]. Computed tomography (CT) using thin-section technique provides superior contrast resolution and can better characterize and localize radiographic abnormalities. CT may be used when radiographic findings are equivocal or absent and clinical suspicion for infection remains high or if complications such as necrotizing infection, empyema, or chest wall involvement are suspected. While certain CT findings can favor infection over alternative diagnoses such as drug toxicity, heart failure, or aspiration, the specificity of CT for identifying the causative organism remains low [1, 7•].

The primary radiologic patterns of infections include ground-glass opacity (GGO), consolidation, masses (3 cm or larger), large and small (< 1 cm) nodules, lymphadenopathy, and infections involving the pleura and chest wall. GGO is defined as increased attenuation of the lung parenchyma without obscuration of the underlying bronchovascular structures [8]. Diffuse GGO may result in poorly defined bronchovascular structures or subtle hazy opacity on chest radiographs, although GGO is frequently occult when less severe. Consolidation is defined as increased and homogenous attenuation of the lung parenchyma that obscures the underlying bronchovascular structures [8].

Small (< 1 cm) pulmonary nodules are classified on CT into perilymphatic, centrilobular, or random distributions; the latter two are commonly associated with infection. Centrilobular nodules can be solid or poorly defined, are relatively evenly distributed, and do not abut the pleura, large bronchovascular structures, or interlobular septa [8].

Table 1 Differential diagnosis of imaging findings in immunocompromised patients

Imaging finding	Common infections	Common noninfectious causes
Ground-glass opacity	<i>Pneumocystis</i> pneumonia	Alveolar hemorrhage
	CMV pneumonia	Lung edema
	Respiratory viral pneumonia	Drug toxicity
Consolidation, masses, and nodules \geq 10 mm	Bacterial pneumonia	Aspiration
	Endemic fungal infection:	Neoplasm
	Histoplasmosis	Lymphoproliferative disorders
	Blastomycosis	
	Coccidioidomycosis	
	Opportunistic fungal infection:	
	Aspergillosis	
	Mucormycosis	
	Cryptococcus	
	Small nodules < 10 mm	Mycobacterial infection
Endemic fungal infection		Metastases
Lymphadenopathy	Endemic fungal infection	Sarcoidosis
	Mycobacterial infection	Metastases
		Lymphoproliferative disorders
CT halo sign	Aspergillosis	Lung carcinoma
	Mucormycosis	Hemorrhagic metastasis
Reversed halo sign		Kaposi sarcoma
	Aspergillosis	Granulomatosis with polyangiitis
	Mucormycosis	Organizing pneumonia
Air crescent sign		Pulmonary infarction
	Aspergillosis	Drug toxicity
	Mucormycosis (less common)	Lung carcinoma
		Intracavitary hemorrhage
		Granulomatosis with polyangiitis

Table 2 Pathogens with common imaging findings in various immunocompromised states

	Ground-glass opacity	Consolidation, masses, nodules ≥ 10 mm	Nodules < 10 mm	Pleural and chest wall infection	Lymphadenopathy
HIV	<i>Pneumocystis</i>	<i>S. pneumoniae</i>	Mycobacteria	<i>M. tuberculosis</i>	Mycobacteria
	CMV	<i>H. influenzae</i>	<i>Coccidioides</i>	<i>S. aureus</i>	<i>H. capsulatum</i>
	<i>H. influenzae</i>	<i>P. aeruginosa</i>	<i>Histoplasma capsulatum</i>	<i>Nocardia</i>	<i>Coccidioides</i>
		<i>S. aureus</i>			
HSCT		<i>Cryptococcus</i>			
		<i>Nocardia</i>			
		<i>Blastomyces dermatitidis</i>			
		<i>Strongyloides stercoralis</i>			
		<i>Aspergillus</i>	<i>Candida</i>		
		<i>Pseudomonas</i>			
		<i>Nocardia</i>			
Solid organ transplant		<i>Legionella</i>			
		<i>H. influenzae</i>			
		<i>Enterobacter</i>			
		<i>Candida</i>			
		<i>S. aureus</i>	Mycobacteria	Bacteria	<i>H. capsulatum</i>
		<i>Legionella</i>	<i>Candida</i>		<i>Coccidioides</i>
		<i>S. pneumoniae</i>	<i>H. capsulatum</i>		Mycobacteria (uncommon)
		<i>H. influenzae</i>			
		<i>Nocardia</i>			
		<i>Aspergillus</i>			
CVID		<i>Cryptococcus</i>			
		<i>Mucorales</i>			
		<i>B. dermatitidis</i>			
CVID		<i>S. pneumoniae</i>	Mycobacteria		
		<i>H. influenzae</i>			

HIV human immunodeficiency virus, HSCT hematopoietic stem cell transplant, CVID common variable immunodeficiency

Centrilobular nodules are a common manifestation of inflammatory or infectious bronchiolitis. Tree-in-bud opacities, highly suggestive of infectious bronchiolitis (Fig. 1), result from filling and distention of terminal bronchioles with debris and secretions and are recognized as centrilobular nodules connected by intervening branching linear opacities [8, 9]. Although first described with mycobacterial infection, tree-in-bud opacities may be caused by a variety of organisms or aspiration. A random distribution of diffuse tiny lung nodules, also known as a miliary pattern, most commonly results from hematogenous dissemination of granulomatous infection, usually tuberculosis or endemic fungus in the setting of cell-mediated immune suppression [1, 3, 9–11•].

Lymphadenopathy is a common manifestation of mycobacterial and endemic fungal infections [6•, 10]. Hilar and mediastinal lymph nodes are most commonly involved. Less frequently, enlarged axillary, supraclavicular, and neck lymph nodes may be present. Noninfectious



Fig. 1 40-year-old male with HIV infection and streptococcal bronchiolitis. HRCT image shows diffuse tree-in-bud opacities and bronchial wall thickening

causes of lymphadenopathy include sarcoidosis, lymphoproliferative disorders, and metastases.

The pleura may be involved in several opportunistic infections, either in isolation or in conjunction with lung involvement. Inflammatory thickening of the visceral and parietal pleura surrounding a pleural fluid collection is known as the split pleura sign on CT and is more conspicuous following intravenous contrast administration (Fig. 2) [9]. The split pleura sign is highly suggestive of empyema but can also occur with noninfectious pleural inflammation.

Chest wall infections are more common in immunocompromised, diabetic, or injured patients and usually result from direct extension from pulmonary or pleural disease rather than direct inoculation of organisms into chest wall tissue. Common organisms causing chest wall infection include *Mycobacterium tuberculosis*, *Actinomyces* spp., *Aspergillus* spp., pyogenic bacteria, and *Nocardia asteroides* complex [12, 13]. CT and MRI better delineate the extent of soft tissue and bone involvement than radiographs or physical exam. Imaging findings of

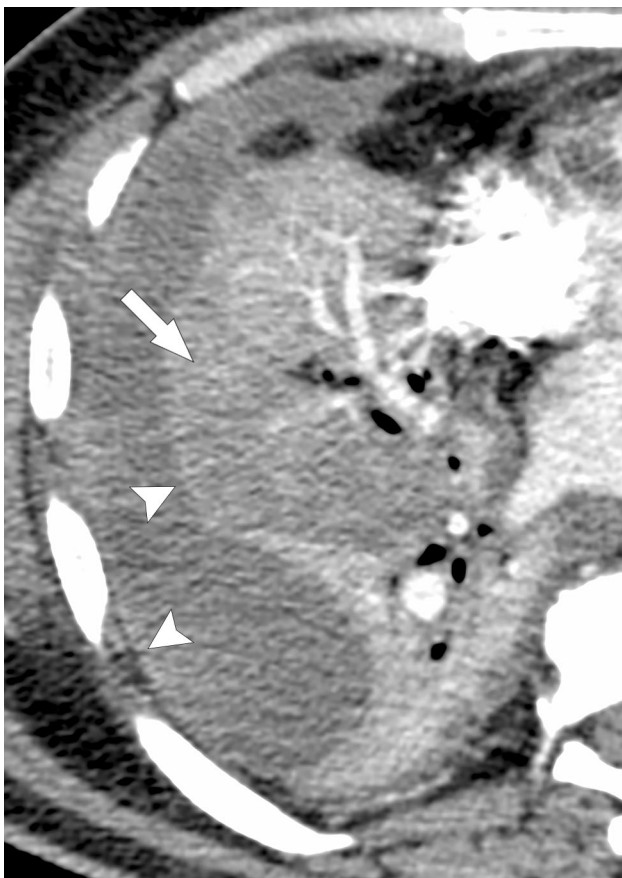


Fig. 2 29-year-old male with staphylococcal empyema. Contrast-enhanced CT image shows a split pleura sign where an exudative effusion separates thickened and enhancing visceral and parietal pleural layers (arrowheads). Adjacent lower-attenuation right lung consolidation representing infection (arrow) is surrounded by homogeneously enhancing atelectasis

chest wall infection include osteolysis, fluid collections, soft tissue stranding, and muscle enlargement with loss of normal fat planes [12–14].

Immunocompromised States

Immunosuppressive regimens and diseases that alter immune function can impair the immune system at one or more pathways including phagocytic, cell-mediated (T lymphocyte), humoral or antibody-mediated (B lymphocyte), complement, and splenic function [1]. Commonly encountered immunocompromised patients include those with HIV/AIDS, hematopoietic stem cell transplant (HSCT) recipients, solid organ transplant recipients, and those with congenital immunodeficiency, especially those with common variable immunodeficiency (CVID). HIV/AIDS patients suffer from T cell dysfunction, and HSCT patients begin with severe immunosuppression and neutropenia and slowly recover neutrophil function, followed by cell-mediated immunity, and finally humoral immunity. Solid organ transplant recipients are at the greatest risk for opportunistic infection early in the posttransplant period with risks decreasing as the intensity of immunosuppressive therapy decreases. Patients with CVID have impaired humoral immunity and are at risk for recurrent sinonasal and pulmonary infections. For all immunosuppressed patients, the underlying immunodeficiency predicts predisposition to specific viral, bacterial, or fungal infections [1, 15].

HIV/AIDS

The Joint United Nations Program on HIV/AIDS estimates that about 36.9 million people are living with HIV infection worldwide [16]. While the use of antiretroviral therapies has significantly reduced the incidence of HIV-associated opportunistic infections, pulmonary infections remain the most common complication in HIV-infected patients and are a major cause of morbidity and mortality. The risk of infections from various opportunistic pathogens depends on the host immune status, specifically CD4 + T-lymphocyte count, and the use of prophylactic therapy.

Community-acquired bacterial pneumonia is the most common infection in HIV-infected patients; common pathogens in order of decreasing frequency include: *Streptococcus pneumoniae*, *Haemophilus influenzae*, and *Staphylococcus aureus*. The incidence of pneumonia increases above that of immunocompetent patients when the CD4+ T-lymphocyte count falls below 400 cells/mm³. The incidence of recurrent bacterial pneumonia and nontuberculous mycobacterial infection increases with further reduction in CD4+ T-lymphocyte count below 300 cells/

mm^3 . *Pneumocystis jirovecii* pneumonia (PJP) typically occurs with CD4^+ T-lymphocyte counts $< 200 \text{ cells}/\text{mm}^3$. With continued decrease of CD4^+ T-lymphocyte counts, particularly $< 100 \text{ cells}/\text{mm}^3$, endemic fungal, viral, and parasitic infections occur with the increasing frequencies.

Radiologic Patterns

Imaging patterns of manifestation of pulmonary infections in HIV/AIDS patients include GGO, consolidation, and nodules in centrilobular, tree-in-bud, and miliary distributions.

GGO

The differential diagnosis of infections causing predominantly GGO in HIV-infected includes *Pneumocystis jirovecii* and cytomegalovirus (CMV). PJP occurs primarily in patients with deficient cell-mediated immunity and is the most common opportunistic infection in patients with AIDS [17]. Patients receiving corticosteroids, antirejection medication, cytotoxic drugs, or other chemotherapy are also at risk for PJP, especially when prophylaxis is not administered. Radiographic findings of PJP include diffuse or upper lung-predominant haziness or small band-like areas of opacity. However, in many patients, findings are subtle, and up to one-third of patients with PJP have normal radiographs [18]. The most common CT manifestation of PJP is patchy or extensive GGO, usually upper lobe predominant (Figs. 3, 4). Consolidation, cysts, nodules, or spontaneous pneumothorax can occur. Clinical clues suggesting PJP as a cause of GGO include elevated serum lactate dehydrogenase, insidious onset of dry cough and dyspnea, and leukopenia [17]. *H. influenzae* infection is also known to mimic PJP imaging findings and should also be considered in HIV patients with bilateral GGO [19]. Common noninfectious causes of GGO in HIV/AIDS patients include lung edema from heart disease and organizing pneumonia related to drug toxicity. Findings favoring lung edema over PJP include basal predominance, interlobular septal thickening, and pleural effusion. Distinguishing drug toxicity from PJP may be more difficult, but CD4^+ T-lymphocyte counts above $200 \text{ cells}/\text{mm}^3$ make drug reaction more likely.

CMV is a herpes virus that infects most people with few or no clinical manifestations. In healthy individuals, the virus can remain dormant for years. However, reactivation of infection can occur in immunocompromised hosts, or less commonly, transmission of dormant virus in the transplanted organ to the recipient. The most common CT findings of pulmonary CMV infection include GGO, which may be associated with consolidation and small nodules (Fig. 5) [20, 21].

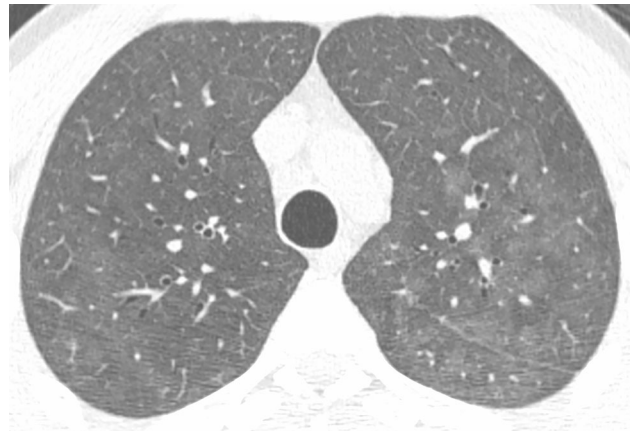


Fig. 3 24-year-old male with AIDS and PJP. HRCT image shows diffuse ground-glass opacity



Fig. 4 26-year-old-male with AIDS and PJP. Coronal reformatted HRCT image shows patchy peribronchial and upper lung-predominant ground-glass opacity. Mild paraseptal emphysema is present

Consolidation, Masses, and Large Nodules ($> 10 \text{ mm}$)

The differential diagnosis of infectious causes of consolidation, masses, and large nodules in patients with HIV infection includes bacterial infection, cryptococcosis, nocardiosis, toxoplasmosis, and endemic fungal infection such as blastomycosis.

Bacterial pneumonia has a broad range of imaging findings, most commonly segmental, lobar, or multilobar consolidation. Large and small nodules with or without cavitation and tree-in-bud opacities can also occur. Pleural effusion is common [19, 22]. Chest radiography is usually

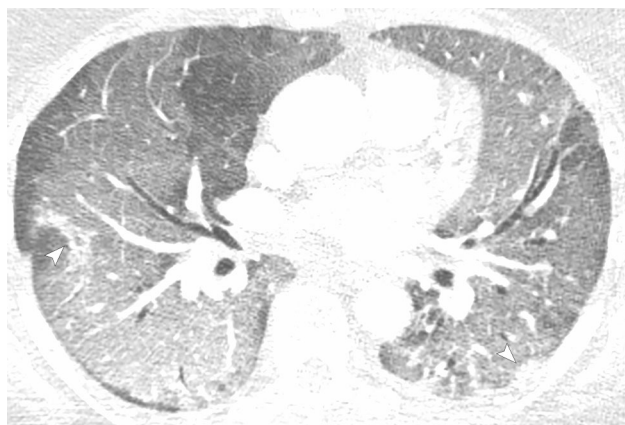


Fig. 5 32-year-old female allogeneic HSCT recipient with CMV infection. HRCT image shows extensive ground-glass opacity with few small foci of consolidation (arrowheads)

sufficient to establish a diagnosis, with CT reserved for equivocal cases or suspected complications.

Nocardia asteroides complex is a group of bacteria found in soil worldwide. Pulmonary nocardiosis is an opportunistic infection affecting patients with deficient cell-mediated immunity including solid organ transplant recipients. Imaging findings include single or multiple nodules, which cavitate in up to one-third of patients, upper lobe-predominant lobar or multilobar consolidation, and pleural involvement including effusion and thickening. Direct extension into the chest wall can also occur. Lymphadenopathy does not usually develop with pulmonary nocardiosis, helping to distinguish it from tuberculosis and opportunistic fungi (Fig. 6) [13, 19, 23]. Actinomycosis, which is associated with poor dentition and aspiration and is not an opportunistic infection, has similar imaging appearances to nocardiosis. However, unlike nocardiosis, dissemination to the central nervous system does not occur with actinomycosis [24].

Cryptococcosis is an opportunistic fungal infection, occasionally affecting immunocompetent patients, caused by *Cryptococcus neoformans* and less often *Cryptococcus gattii*. It primarily affects patients with cell-mediated immunity deficiency, including those with HIV and solid organ transplants. Pulmonary cryptococcosis most commonly presents as solitary or multiple nodules or masses (cryptococcomas) (Fig. 7) [25]. In a retrospective analysis of 42 patients with pulmonary cryptococcosis (33 immunocompetent and 9 immunocompromised), mass-like and peribronchial consolidation was more common in immunocompromised patients, whereas solitary nodules occurred more frequently in immunocompetent patients [26]. In the authors' experience, cryptococcomas in immunocompromised patients usually are large with well-defined walls and lack surrounding ground-glass opacity.

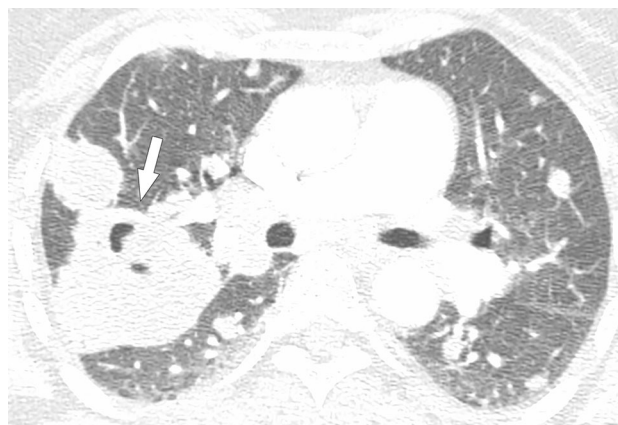


Fig. 6 42-year-old female who developed nocardiosis while being treated with chemotherapy for astrocytoma. HRCT image shows multiple bilateral large nodules and dense consolidation with cavitation in the right upper lobe (arrow)

Blastomyces dermatitidis is an endemic fungus found in the central and southeastern United States with the highest rates in the upper Midwest. Blastomycosis occurs with similar incidences in immune competent and immunocompromised patients, although the severity of infection is often worse in the latter. About 25% of AIDS-related cases can result from reactivation of a dormant infection. [27] The most common imaging findings are patchy or confluent consolidation, masses, and nodules (Fig. 8) [10]. Pleural effusion and lymphadenopathy are uncommon, helping to distinguish blastomycosis from bacterial infection. Up to 20% of patients with AIDS present with severe pulmonary disease including hematogenous dissemination (miliary pattern of lung nodules) (Fig. 9) or acute respiratory distress syndrome [27]. Other findings favoring blastomycosis over other infections include skin, central nervous system, and skeletal involvement.

While less-frequent, immunocompromised hosts can acquire severe parasitic infections. Toxoplasmosis is the most common parasitic infection associated with HIV infection and primarily involves the central nervous system. Pneumonia is the second most common presentation [23]. Pulmonary manifestations include diffuse bilateral opacities with or without nodules [23, 28, 29].

Transient eosinophilic pneumonia (Löfller syndrome) is an acute inflammatory response commonly occurring in response to infections with *Ascaris lumbricoides* or *Strongyloides stercoralis*. Imaging findings most commonly involve transient or migratory consolidation and less commonly pulmonary nodules, subpleural linear opacities, or abscess [3, 30, 31]. *Strongyloides* infection, although rare, may also occur in other immunocompromised states including hematologic malignancies (Fig. 10).

Noninfectious causes of consolidation, masses, and large nodules include post-transplant lymphoproliferative

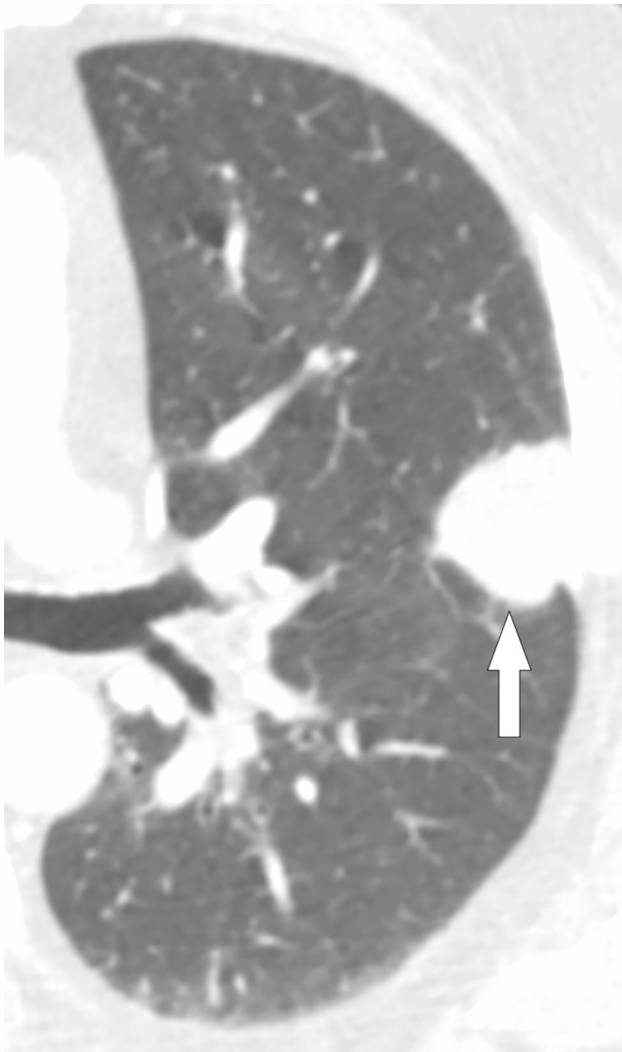


Fig. 7 54-year-old male liver transplant recipient with cryptococcal infection. HRCT image shows a left lower lobe mass with well-defined margins (arrow). Note the lack of surrounding ground-glass opacity, favoring cryptococcosis over angioinvasive fungal infection

disorder, recurrence or progression of hematologic malignancies such as lymphoma or myeloid sarcoma, lung carcinoma, and metastases. A slower temporal evolution of these findings may favor a noninfectious cause, but tissue sampling is usually required to establish a diagnosis.

Small Nodules < 10 mm

A miliary pattern of micronodules most commonly results from disseminated mycobacterial and endemic fungal infections (Fig. 11) [1, 3, 9–11]. In the authors' experience, the nodules of miliary tuberculosis are frequently more profuse and smaller than those associated with miliary fungal infection. Furthermore, travel and immigration history may help favor one infection over another.

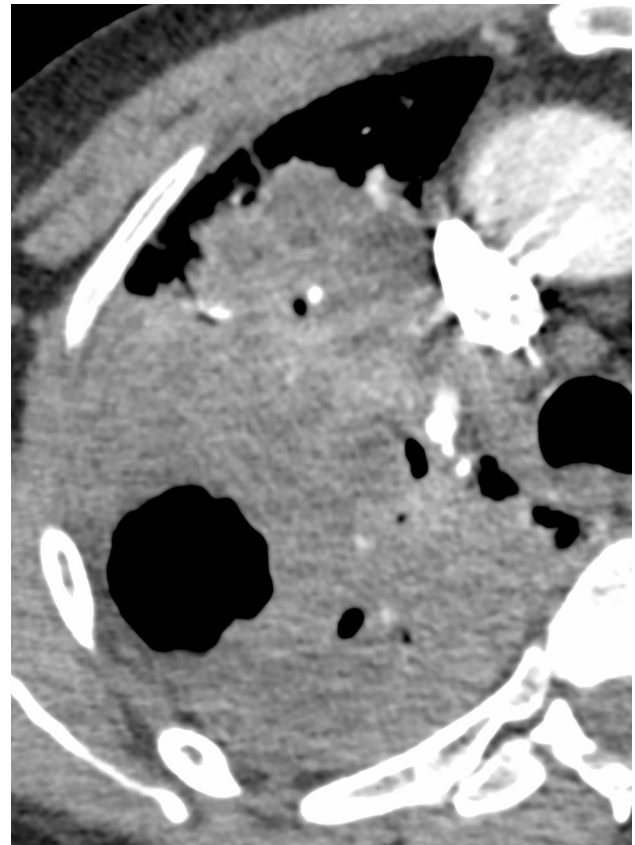


Fig. 8 52-year-old-male liver transplant recipient with blastomycosis. HRCT shows extensive right upper lobe consolidation with central cavitation. Pleural effusion, if any, is minimal, favoring fungal infection over bacterial

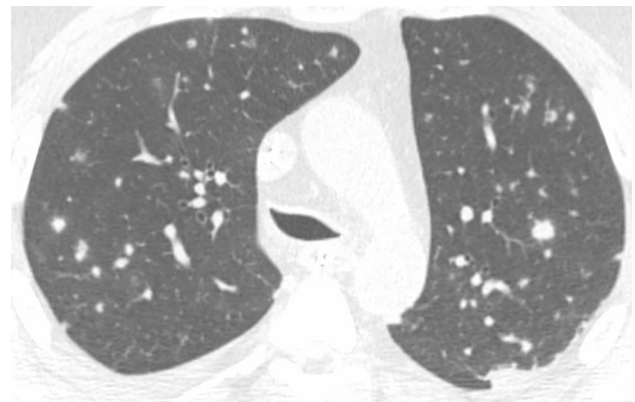


Fig. 9 47-year-old male kidney and pancreas transplant recipient with blastomycosis. HRCT image shows diffuse small and large nodules in random distribution. The heterogeneity of nodule size favors endemic fungal infection over mycobacterial infection. Note flattening of the anterior tracheal wall as a result of tracheomalacia

Disseminated tuberculosis usually occurs in HIV-infected patients with CD4 + T-lymphocyte counts below 200 cells/mm³. Patients are at risk for disseminated *Mycobacterium avium* complex (MAC) infection when

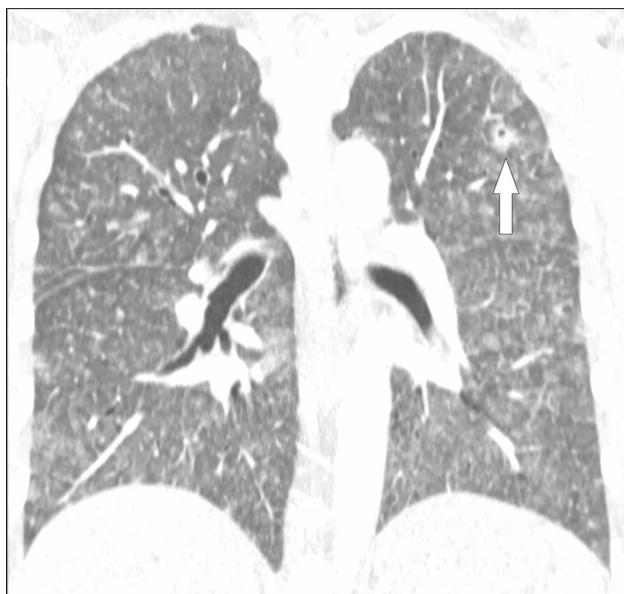


Fig. 10 52-year-old male with leukemia and *Strongyloides* infection. Coronal-reformatted HRCT image shows diffuse ground-glass opacity and solid nodules and a cavitary nodule in the left upper lobe (arrow). Courtesy of J. David Godwin, M.D. (Seattle, WA)

CD4 + T-lymphocyte counts fall below 50 cells/mm³ [28]. *Mycobacterium xenopi* and *Mycobacterium kansasii* also cause pulmonary disease [22], with the former also reported to cause disseminated disease [1].

Coccidioides immitis and *Coccidioides posadasii* are endemic in the southwestern United States, San Joaquin valley of California, northern Mexico, and central Oregon and Washington [32]. Immunocompetent and immunocompromised patients are affected, but disseminated disease is more common in immunocompromised patients. Imaging findings include multilobar consolidation, nodules



Fig. 11 52-year-old male kidney transplant recipient with disseminated tuberculosis. HRCT image illustrates the random distribution (miliary pattern) with an area of clustering near the right hilum

with or without cavities, and lymphadenopathy [11•]. Pleural effusion can also be present [11•]. Disseminated disease resembles histoplasmosis with a miliary pattern of lung nodules (Fig. 12). Other clues to the diagnosis include arthralgia, conjunctivitis, and skin rash; and travel history can be valuable.

Histoplasma capsulatum is a dimorphic fungus endemic to the Midwestern and Eastern United States, particularly along the Mississippi and Ohio River valleys and around the Great Lakes. Histoplasmosis affects 2% of the AIDS population [22], likely higher in endemic areas. Whereas histoplasmosis is nearly always a clinically silent, self-limited infection in immunocompetent patients, immunocompromised patients are at risk for disseminated infection with a miliary pattern of lung nodules with or without thoracic lymphadenopathy. Consolidation is uncommon, and cavitation is rare (Fig. 10), helping distinguish histoplasmosis from blastomycosis and other infections.

Noninfectious causes of numerous small nodules include metastases and drug-induced granulomatous inflammation (particularly related to TNF- α inhibitors). Nodules from hematogenously disseminated metastases vary somewhat in size and have a random, basal-predominant distribution, whereas nodules from drug-induced granulomatous inflammation have a more perilymphatic distribution, similar to that of sarcoidosis.

Lymphadenopathy

AIDS patients with mycobacterial infections may have normal to abnormally enlarged lymph nodes. Ketai et al. showed that 60-75% of pulmonary tuberculosis patients infected with HIV had abnormally enlarged thoracic lymph nodes [6••]. Disseminated MAC infection can manifest as multifocal low-attenuation lymphadenopathy.

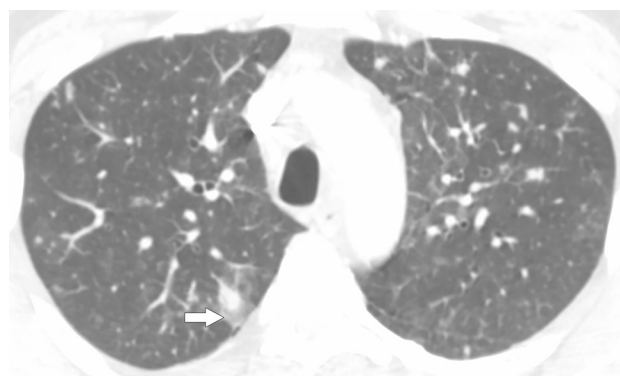


Fig. 12 47-year-old male with AIDS and disseminated coccidioidomycosis. HRCT image shows multiple small and large nodules with a single right upper lobe nodule surrounded by ground-glass opacity (arrow). Note the heterogeneity of nodule size, a finding more typical of miliary fungal infection

Histoplasmosis and coccidioidomycosis are the two most common endemic mycoses causing intrathoracic lymphadenopathy [1]. Noninfectious causes of lymphadenopathy in HIV-infected patients include metastases, lymphoma, and immune reconstitution inflammatory syndrome.

Pleura and Chest Wall Infections

Pleural effusion or empyema can develop with tuberculosis and less commonly with non-mycobacterial infections such as *S. aureus* [1]. Nocardiosis may cause pleural thickening [1] and infrequently pleural effusions [13]. Chest wall invasion (empyema necessitatis) primarily occurs in HIV-infected patients with tuberculosis [12].

Hematopoietic Stem Cell Transplant (HSCT)/Bone Marrow Transplant

HSCT is used primarily to treat hematologic malignancies by means of chemotherapy for myeloablation, eradicating malignant cells with total body irradiation, and infusing donor (allogeneic) or patient (autologous) stem cells for hematopoiesis [33]. Unlike solid organ transplant recipients, HSCT recipients have a characteristic sequence of immunosuppression as engraftment occurs and hematopoiesis ensues. With normal engraftment, neutropenia resolves within 2–4 weeks, while cellular and humoral immunity can take 6–12 months to recover [33]. In the pre-engraftment period (days 0–30), characterized by neutropenia, fungal infections are more frequent, although the incidence of invasive aspergillosis as well as bacterial infections has decreased with the increased prophylaxis and empiric antibiotic usage, respectively [1]. In the early post-transplantation period (days 31–100), infections with CMV and *Aspergillus* are most common. PJP is now rare following HSCT because of routine prophylaxis. Complications in the late phase (days 101–1 year) arise primarily in patients with graft-versus-host disease (GVHD), which affects approximately half of allogeneic HSCT recipients. Not only does GVHD directly inhibit immune function but also its treatment with corticosteroids places patients at greater risk for infection. Common respiratory viruses that cause late-phase complications are adenovirus, respiratory syncytial virus, varicella-zoster virus, and parainfluenza virus [1]. Fungal infections include aspergillosis and mucormycosis.

Radiologic Patterns

GGO

Extensive GGO should suggest CMV in the early-phase and community-acquired respiratory viruses in the late phase. Additional findings favoring viral infection include centrilobular nodules, bronchial wall thickening, and peribronchial consolidation (Fig. 13) [21]. Noninfectious causes should also be considered, particularly during early engraftment, and include edema from acute kidney injury, acute lung injury from graft-versus-host disease and idiopathic pneumonia syndrome, and hemorrhage from drug toxicity or thrombocytopenia.

Consolidation, Masses, and Large Nodules (> 10 mm)

Neutropenia is the greatest risk factor for invasive aspergillosis, although aspergillosis can occur in all three phases. On CT, angioinvasive aspergillosis manifests as one or more nodules or masses and areas of wedge-shaped consolidation. GGO surrounding a lung nodule or mass (CT halo sign), while being not pathognomonic, is highly suggestive in the appropriate setting [8, 34]. The ground-glass halo corresponds to hemorrhage, and the higher attenuation center is infarcted lung [35]. The CT halo sign has also been reported with candidiasis, CMV, HSV, tuberculosis, cryptococcosis, and mucormycosis and may occur with noninfectious causes such as primary malignancy, hemorrhagic metastasis, or Kaposi sarcoma [9, 35, 36]. The air crescent sign results from retraction of infarcted and necrotic lung from the surrounding hemorrhagic parenchymal rim (Fig. 14) [35]. It is associated with a good prognosis and indicates recovering immunity with resolution of neutropenia [8, 34]. The air crescent sign is the most commonly associated with aspergillosis but has been reported in respect of other conditions such as tuberculosis, granulomatosis with polyangiitis, intracavitary hemorrhage, and lung cancer [8]. Airway invasive aspergillus accounts for only 10% of aspergillus infections and is characterized by peribronchial consolidation and small airway-centric nodules [1] (Figs. 15, 16).

Pulmonary mucormycosis is caused by invasive infection from fungi in the *Mucorales* order, most commonly *Mucor* and *Rhizopus*. Patients with neutropenia and other cell-mediated immunodeficiencies are at greatest risk. Mucormycosis is difficult to treat and has a high mortality rate with CT manifestations similar to angioinvasive aspergillosis (Fig. 17), although in the authors' experience, masses and consolidation tend to be larger than with *Aspergillus*, and progression is more rapid. In a retrospective study of 20 immunocompromised patients with histologically proven pulmonary mucormycosis, the most

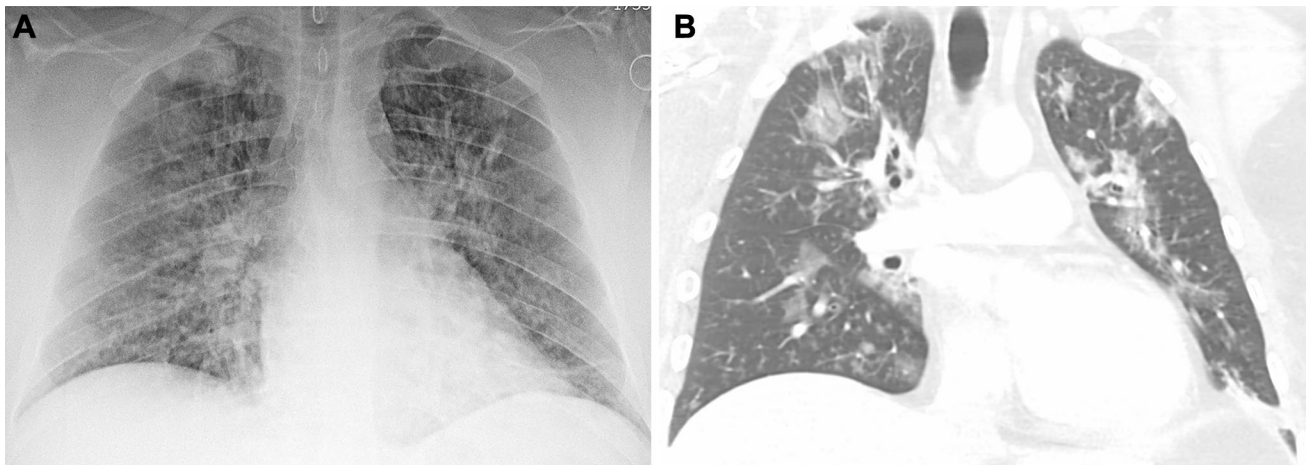


Fig. 13 57-year-old female HSCT recipient with RSV infection. **a** PA radiograph shows poorly defined nodules and bronchial wall thickening. **b** Coronal reformatted HRCT image shows bilateral patchy ground-glass opacities, scattered micronodules, and tree-in-bud opacities

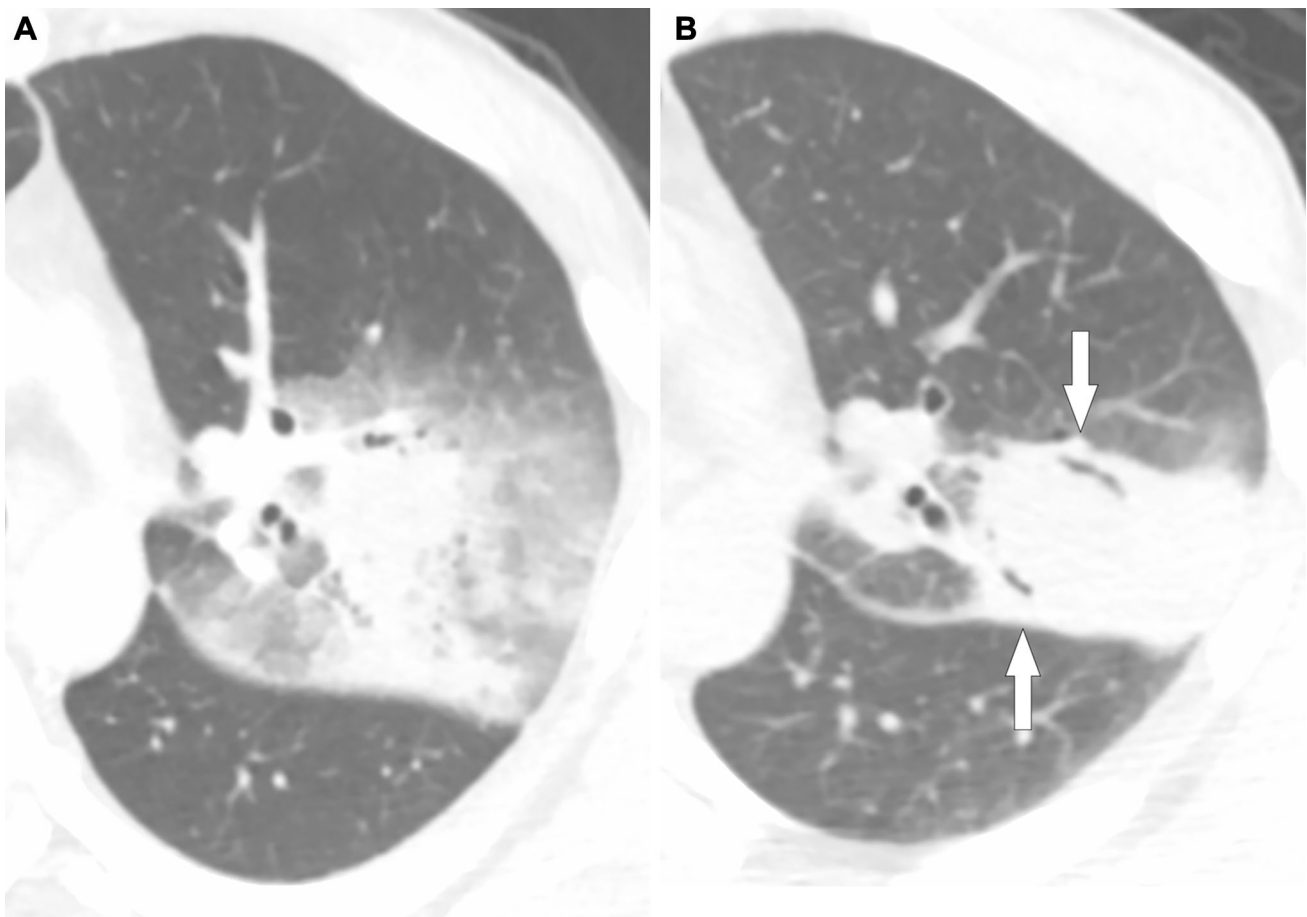


Fig. 14 52-year-old male with invasive aspergillosis following HSCT for chronic myelogenous leukemia. **a** HRCT image shows dense consolidation in the left upper lobe with surrounding ground-glass opacity (CT halo sign). **b** HRCT image obtained 20 days later

shows dense left upper lobe consolidation with development of internal crescentic foci of gas (arrows) (air crescent sign). Courtesy of Travis S. Henry, M.D. (San Francisco, CA)

common CT finding was consolidation with large nodules or masses including the CT halo sign [37]. The presence of

a bird's nest sign, characterized by peripheral consolidation with central low attenuation, cavitation, linear intersecting



Fig. 15 57-year-old female with acute myelogenous leukemia and *Rhizopus* infection. Contrast-enhanced CT image shows a complex cavitory mass containing a fluid level (arrow) in the right upper lobe. Chest wall extension is characterized by a fluid collection (asterisk) between the serratus anterior and the pectoralis muscles. Notice the loss of normal tissue planes and stranding of subcutaneous fat in the right lateral chest wall

stranding, and GGO should strongly suggest invasive mucormycosis (Fig. 18) [9, 38]. With resolving neutropenia, the reversed halo sign, central necrosis, and air crescent sign can develop [37, 39]. The reversed halo or atoll sign is characterized by peripheral consolidation and central GGO, often reflecting peripheral organizing pneumonia with central alveolar cellular debris and septal inflammation. The reversed halo sign can also occur with other infections including aspergillosis, less tuberculosis, PJP, and paracoccidioidomycosis. Noninfectious causes include organizing pneumonia, pulmonary infarction, sarcoidosis, granulomatosis with polyangiitis, lymphomatoid granulomatosis, lipoid pneumonia, and lepidic-predominant lung adenocarcinoma [8, 35, 39].

Small Nodules < 10 mm

Candida albicans cause fungal pneumonia in neutropenic patients and patients with hematologic malignancies, but invasive disease is atypical. *Candida* infections primarily occur in allogeneic HSCT recipients with prolonged neutropenia and increased age [40]. CT findings usually include multiple lung nodules and patchy GGO consolidation. The CT halo sign may be present [41]. Numerous small lung nodules resembling a miliary pattern and cavitation can also occur [40].

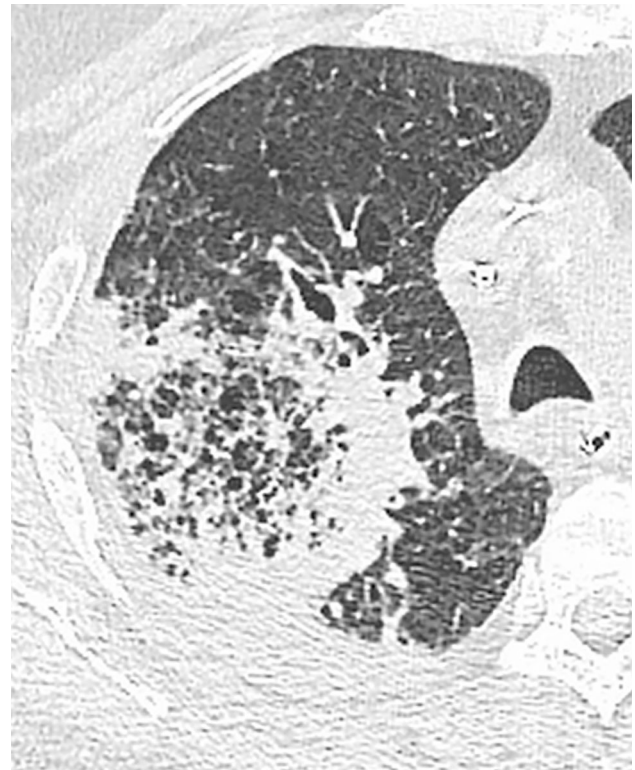


Fig. 16 66-year-old male with multiple myeloma with mucormycosis. HRCT image shows right upper lobe consolidation with central cavitations, ground-glass opacity, and linear intersecting and patchy opacities depicting a bird's nest sign. Courtesy of Julie E. Takasugi, M.D. (Seattle, WA)



Fig. 17 51-year-old male kidney transplant recipient with HSV pneumonia. Coronal reformatted HRCT image shows upper lobe-predominant ground-glass opacity and right upper lobe consolidation

Solid Organ Transplant

While the number of solid organ transplants continue to increase, the incidence of post-transplant infections has decreased with routine prophylaxis and improved

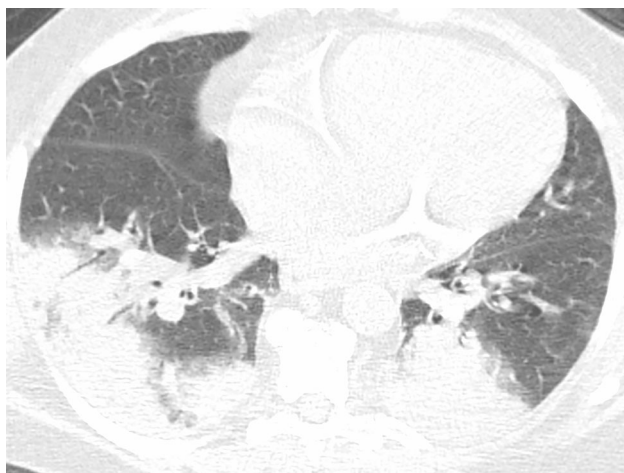


Fig. 18 56-year-old female kidney transplant recipient with *Legionella* pneumonia. HRCT image shows multifocal consolidation in the lower lobes. A small amount of peripheral ground-glass opacity is also present. While the distribution would also be typical for aspiration, the lack of airway debris and tree-in-bud opacities makes it less likely

immunosuppressive regimens. Nevertheless, pulmonary infections remain common in these patients and are most frequent at 4–6 months after transplant [40]. Hospital-acquired pneumonia occurs primarily in perioperative period and includes gram-negative bacteria, *Staphylococcus aureus*, and *Legionella* spp. [1]. After 6 months, community-acquired respiratory tract infections become more common. *S. pneumoniae* is the most common infection in heart–lung and lung transplant recipients [1, 40]. Nocardiosis occurs in only up to 2% of solid organ transplant recipients, presumably as a consequence of routine prophylaxis with sulfa antibiotics for PJP [1].

Tuberculosis occurs in fewer than 2% of solid organ transplant recipients in the U.S. with higher rates in endemic regions [42]. Nontuberculous mycobacterial infection is less common than tuberculosis in solid organ transplant recipients and usually develops much later after transplant [43].

Solid organ transplant patients are predisposed to various viral infections including CMV and community-acquired respiratory viruses. The most common fungal infections in this patient population include invasive aspergillosis and candidiasis, occurring in 1–15% [44]. Cryptococcosis is reported in approximately 8%, and mucormycosis affects about 2% of patients [44]. Endemic fungal infections in this population are limited to their respective geographic areas. *Pneumocystis jirovecii* is a less-common complication after solid organ transplant and primarily affects lung transplant recipients [45].

Radiologic Patterns

GGO

Chest radiographic findings may be subtle or occult with viral infection. CT is more sensitive, showing diffuse or patchy GGO often with tiny nodules and occasionally patchy areas of consolidation (Fig. 17). Pleural effusion and septal thickening in addition to GGO should raise the question of lung edema, particularly in patients with drug-induced kidney injury. Patchy ground-glass opacity can also reflect acute rejection in lung transplant recipients.

Consolidation, Masses, Large Nodules > 10 mm

Hospital and community-acquired bacterial pneumonias classically manifest as multifocal consolidation with segmental or lobar distribution (Fig. 18). Nocardiosis and aspergillosis should be strongly considered when large nodules with or without the CT halo sign are present.

Congenital Immunocompromised State

Most primary immunodeficiency states involve humoral deficiency and include common variable immunodeficiency (CVID), IgA deficiency, and X-linked agammaglobulinemia [31]. Patients with CVID present when 20–40 years old with a mean age of 29 years old [46, 47•]. CVID involves reduced levels of immunoglobulins, and up to 50% of patients have T-lymphocyte abnormalities [47•]. Infections most commonly result from *H. influenzae* and *S. pneumoniae* [46, 47•]. Opportunistic infections are rare and include PJP, CMV, and mycobacterial infection [47•].

Radiologic Pattern

The most commonly reported imaging finding in CVID is bronchiectasis [46]. Lobar or segmental consolidation with mediastinal or hilar lymphadenopathy and cavitation can occur with acute bacterial pneumonia [47•]. Centrilobular nodules with tree-in-bud opacities are typically from viral or encapsulated bacterial infections [47•]. Granulomatous-lymphocytic interstitial lung disease (GL-ILD) is a diffuse lung process affecting patients with CVID that may be related to human herpesvirus 8 [48]. The combination of numerous small lung nodules, mediastinal lymphadenopathy, and splenomegaly is highly suggestive of GL-ILD and can help distinguish it from infection.

Conclusions

Chest infections remain major contributors to morbidity and mortality in immunocompromised patients. Imaging plays a central role in the diagnosis of infection. Although there is significant overlap of radiologic manifestations among a variety of pulmonary infections, the presence or absence of certain findings can help the radiologist narrow the differential diagnosis, especially when clinical information such as type, degree, and duration of immunosuppression as well as travel and environmental exposures is considered. Finally, the radiologist should always be aware of noninfectious processes such as malignancy and drug toxicity, which can mimic the imaging manifestations of infection.

Compliance with Ethical Guidelines

Conflict of interest Ruchi Sharma, Jeffrey P. Kanne, Maria D. Martin, and Christopher A. Meyer, with each declaring no potential conflicts of interest.

Human and Animal Rights and Informed Consent This article does not contain any studies involving human or animal subjects performed by any of the authors.

References

Recently published papers of particular interest have been highlighted as:

- Of importance
- Of major importance

1. Ahuja J, Kanne JP. Thoracic infections in immunocompromised patients. *Radiol Clin N Am*. 2014;52(1):121–36. <https://doi.org/10.1016/j.rcl.2013.08.010>.
2. George MP, Masur H, Norris KA, Palmer SM, Clancy CJ, McDyer JF. Infections in the Immunosuppressed Host. *Ann Am Thorac Soc*. 2014;11(Suppl 4):S211–20. <https://doi.org/10.1513/AnnalsATS.201401-038PL>.
3. Rali P, Veer M, Gupta N, Singh AC, Bhanot N. Opportunistic pulmonary infections in immunocompromised hosts. *Crit Care Nurs Q*. 2016;39(2):161–75. <https://doi.org/10.1097/CNQ.000000000000109>.
4. Godbole G, Gant V. Respiratory tract infections in the immunocompromised. *Curr Opin Pulm Med*. 2013;19(3):244–50. <https://doi.org/10.1097/MCP.0b013e32835f82a9>.
5. Buckley RH. Immunodeficiency diseases. *JAMA*. 1987;258(20):2841–50.
6. •• Ketai L, Jordan K, Busby KH. Imaging infection. *Clin Chest Med*. 2015;36(2):197–217, viii. <https://doi.org/10.1016/j.ccm.2015.02.005>. *Important review article on principles of imaging infection with a clinical approach.*
7. • Dwivedi A, Kumar RR, Sharma A, Pannu SK. Role of HRCT chest in post stem cell transplant recipients suspected of pulmonary complications. *J Clin Diagn Res*. 2016;10(11):TC18–TC23. <https://doi.org/10.7860/jcdr/2016/24387.8885>. *Discussion of the role of HRCT in HSCT patients.*
8. Hansell DM, Bankier AA, MacMahon H, McLoud TC, Muller NL, Remy J. Fleischner Society: glossary of terms for thoracic imaging. *Radiology*. 2008;246(3):697–722. <https://doi.org/10.1148/radiol.2462070712>.
9. Walker CM, Abbott GF, Greene RE, Shepard JA, Vummidi D, Digumarthy SR. Imaging pulmonary infection: classic signs and patterns. *AJR Am J Roentgenol*. 2014;202(3):479–92. <https://doi.org/10.2214/AJR.13.11463>.
10. Chong S, Lee KS, Yi CA, Chung MJ, Kim TS, Han J. Pulmonary fungal infection: imaging findings in immunocompetent and immunocompromised patients. *Eur J Radiol*. 2006;59(3):371–83. <https://doi.org/10.1016/j.ejrad.2006.04.017>.
11. • Orlowski HLP, McWilliams S, Mellnick VM, Bhalla S, Lubner MG, Pickhardt PJ et al. Imaging spectrum of invasive fungal and fungal-like infections. *RadioGraphics*. 2017;37(4):1119–34. <https://doi.org/10.1148/rg.2017160110>. *This review article includes a discussion of invasive fungal infections in the chest.*
12. Chelli Bouaziz M, Jelassi H, Chaabane S, Ladeb MF, Ben Miled-Mrad K. Imaging of chest wall infections. *Skelet Radiol*. 2009;38(12):1127–35. <https://doi.org/10.1007/s00256-008-0636-z>.
13. Kanne JP, Yandow DR, Mohammed TL, Meyer CA. CT findings of pulmonary nocardiosis. *AJR Am J Roentgenol*. 2011;197(2):W266–72. <https://doi.org/10.2214/AJR.10.6208>.
14. Boruah DK, Sanyal S, Sharma BK, Prakash A, Dhingani DD, Bora K. Role of cross sectional imaging in isolated chest wall tuberculosis. *J Clin Diagn Res*. 2017;11(1):TC01–TC6. <https://doi.org/10.7860/jcdr/2017/23522.9185>.
15. Figueroa JE, Densen P. Infectious diseases associated with complement deficiencies. *Clin Microbiol Rev*. 1991;4(3):359–95.
16. • Huang L, Morris A, Crothers K. Pulmonary complications of HIV infection. *Semin Respir Crit Care Med*. 2016;37(02):145–6. <https://doi.org/10.1055/s-0036-1579582>. *This article includes discussion of infections in patients with HIV/AIDS.*
17. Kanne JP, Yandow DR, Meyer CA. Pneumocystis jiroveci pneumonia: high-resolution CT findings in patients with and without HIV infection. *AJR Am J Roentgenol*. 2012;198(6):W555–61. <https://doi.org/10.2214/AJR.11.7329>.
18. Kuhlman JE. Imaging pulmonary disease in AIDS: state of the art. *Eur Radiol*. 1999;9(3):395–408. <https://doi.org/10.1007/s003300050682>.
19. Chou S-HS, Prabhu SJ, Crothers K, Stern EJ, Godwin JD, Pipavath SN. Thoracic diseases associated with HIV infection in the era of antiretroviral therapy: clinical and imaging findings. *Radiographics*. 2014;34(4):895–911. <https://doi.org/10.1148/rg.344130115>.
20. Gasparetto EL, Ono SE, Escuissato D, Marchiori E, Roldan L, Marques HL, et al. Cytomegalovirus pneumonia after bone marrow transplantation: high resolution CT findings. *Br J Radiol*. 2004;77(921):724–7. <https://doi.org/10.1259/bjr/70800575>.
21. Miller WT Jr, Shah RM. Isolated diffuse ground-glass opacity in thoracic CT: causes and clinical presentations. *AJR Am J Roentgenol*. 2005;184(2):613–22. <https://doi.org/10.2214/ajr.184.2.01840613>.
22. Zheng X, Zhang G. Imaging pulmonary infectious diseases in immunocompromised patients. *Radiol Infect Dis*. 2014;1(1):37–41. <https://doi.org/10.1016/j.jrid.2014.11.001>.
23. Benito N, Moreno A, Miro JM, Torres A. Pulmonary infections in HIV-infected patients: an update in the 21st century. *Eur Respir J*. 2012;39(3):730.
24. Yildiz O, Doganay M. Actinomycoses and Nocardia pulmonary infections. *Curr Opin Pulm Med*. 2006;12(3):228–34. <https://doi.org/10.1097/01.mcp.0000219273.57933.48>.
25. Xie LX, Chen YS, Liu SY, Shi YX. Pulmonary cryptococcosis: comparison of CT findings in immunocompetent and

- immunocompromised patients. *Acta Radiol.* 2015;56(4):447–53. <https://doi.org/10.1177/0284185114529105>.
26. Wang S-y, Chen G, Luo D-l, Shao D, Liu E-t, Sun T et al. 18 F-FDG PET/CT and contrast-enhanced CT findings of pulmonary cryptococcosis. *Eur. J. Radiol.* 2017;89:140–8. <https://doi.org/10.1016/j.ejrad.2017.02.008>.
 27. Smith JA, Gauthier G. New developments in blastomycosis. *Semin Respir Crit Care Med.* 2015;36(05):715–28. <https://doi.org/10.1055/s-0035-1562898>.
 28. Pupaibool J, Limper AH. Other HIV-associated pneumonias. *Clin Chest Med.* 2013;34(2):243–54. <https://doi.org/10.1016/j.ccm.2013.01.007>.
 29. Velásquez JN, Ledesma BA, Nigro MG, Vittar N, Rueda N, De Carolis L, et al. Pulmonary toxoplasmosis in human immunodeficiency virus-infected patients in the era of antiretroviral therapy. *Lung India.* 2016;33(1):88–91. <https://doi.org/10.4103/0970-2113.173063>.
 30. Price M, Gilman MD, Carter BW, Sabloff BS, Truong MT, Wu CC. Imaging of eosinophilic lung diseases. *Radiol Clin N Am.* 2016;54(6):1151–64. <https://doi.org/10.1016/j.rcl.2016.05.008>.
 31. Daltro P, Santos EN, Gasparetto TD, Ucar ME, Marchiori E. Pulmonary infections. *Pediatr Radiol.* 2011;41(Suppl 1):S69–82. <https://doi.org/10.1007/s00247-011-2012-8>.
 32. Stockamp NW, Thompson GR 3rd. Coccidioidomycosis. *Infect Dis Clin N Am.* 2016;30(1):229–46. <https://doi.org/10.1016/j.idc.2015.10.008>.
 33. Tanaka N, Kunihiro Y, Yujiri T, Ando T, Gondo T, Kido S, et al. High-resolution computed tomography of chest complications in patients treated with hematopoietic stem cell transplantation. *Jpn J Radiol.* 2011;29(4):229–35. <https://doi.org/10.1007/s11604-010-0544-8>.
 34. Marom EM, Kontoyiannis DP. Imaging studies for diagnosing invasive fungal pneumonia in immunocompromised patients. *Curr Opin Infect Dis.* 2011;24(4):309–14. <https://doi.org/10.1097/QCO.0b013e328348b2e1>.
 35. • Raju S, Ghosh S, Mehta AC. Chest CT Signs in Pulmonary Disease: A Pictorial Review. *Chest.* 2017;151(6):1356–74. <https://doi.org/10.1016/j.chest.2016.12.033>. *Illustrates many of the signs of pulmonary infection discussed in this manuscript.*
 36. Alves GR, Marchiori E, Irion K, Nin CS, Watte G, Pasqualotto AC, et al. The halo sign: HRCT findings in 85 patients. *J Bras Pneumol.* 2016;42(6):435–9. <https://doi.org/10.1590/S1806-37562015000000029>.
 37. • Nam BD, Kim TJ, Lee KS, Kim TS, Han J, Chung MJ. Pulmonary mucormycosis: serial morphologic changes on computed tomography correlate with clinical and pathologic findings. *Eur Radiol.* 2017. <https://doi.org/10.1007/s00330-017-5007-5>. *Discusses CT findings of pulmonary mucormycosis.*
 38. Jung J, Kim MY, Lee HJ, Park YS, Lee SO, Choi SH et al. Comparison of computed tomographic findings in pulmonary mucormycosis and invasive pulmonary aspergillosis. *Clin. Microbiol. Infect.* 2015;21(7):684.e11–.e18. <https://doi.org/10.1016/j.cmi.2015.03.019>.
 39. Marchiori E, Zanetti G, Hochhegger B, Irion KL, Carvalho AC, Godoy MC. Reversed halo sign on computed tomography: state-of-the-art review. *Lung.* 2012;190(4):389–94. <https://doi.org/10.1007/s00408-012-9392-x>.
 40. Franquet T. High-resolution computed tomography (HRCT) of lung infections in non-AIDS immunocompromised patients. *Eur Radiol.* 2006;16(3):707–18. <https://doi.org/10.1007/s00330-005-0008-1>.
 41. Franquet T, Müller NL, Lee KS, Oikonomou A, Flint JD. Pulmonary candidiasis after hematopoietic stem cell transplantation: thin-section CT findings. *Radiology.* 2005;236(1):332–7. <https://doi.org/10.1148/radiol.2361031772>.
 42. Singh N, Paterson DL. Mycobacterium tuberculosis infection in solid-organ transplant recipients: impact and implications for management. *Clin Infect Dis.* 1998;27(5):1266–77.
 43. Queipo JA, Broseta E, Santos M, Sanchez-Plumed J, Budia A, Jimenez-Cruz F. Mycobacterial infection in a series of 1261 renal transplant recipients. *Clin Microbiol Infect.* 2003;9(6):518–25.
 44. Goetz ME, Evans RA, Rendulic T. Opportunistic pulmonary infections in the solid organ transplant recipient: a focus on drug therapy. *Crit Care Nurs Q.* 2017;40(4):399–413. <https://doi.org/10.1097/CNQ.0000000000000176>.
 45. Gordon SM, LaRosa SP, Kalmadi S, Arroliga AC, Avery RK, Truesdell-LaRosa L, et al. Should prophylaxis for *Pneumocystis carinii* pneumonia in solid organ transplant recipients ever be discontinued? *Clin Infect Dis.* 1999;28(2):240–6. <https://doi.org/10.1086/515126>.
 46. Thickett KM, Kumararatne DS, Banerjee AK, Dudley R, Stableforth DE. Common variable immune deficiency: respiratory manifestations, pulmonary function and high-resolution CT scan findings. *QJM: Int J Med.* 2002;95(10):655–62. <https://doi.org/10.1093/qjmed/95.10.655>.
 47. • Cereser L, Girometti R, d'Angelo P, De Carli M, De Pellegrin A, Zuiani C. Humoral primary immunodeficiency diseases: clinical overview and chest high-resolution computed tomography (HRCT) features in the adult population. *Clin Radiol.* 2017;72(7):534–42. <https://doi.org/10.1016/j.crad.2017.03.018>. *Includes discussion of imaging findings of patients with CVID.*
 48. Park JH, Levinson AI. Granulomatous-lymphocytic interstitial lung disease (GLILD) in common variable immunodeficiency (CVID). *Clin Immunol.* 2010;134(2):97–103. <https://doi.org/10.1016/j.clim.2009.10.002>.